MAGNETIC FIELD ANNIHILATION OF IMPULSIVE CURRENT SHEETS

INTERIM SCIENTIFIC-PROGRESS REPORT

18706-6001-T0-00

MAY 31, 1972

Prepared for

AIR FORCE OFFICE OF SCIENTIFIC RESEARCH
1400 WILSON BOULEVARD
ARLINGTON, VIRGINIA 22209
CONTRACT NO. F44620-C-0031

TRW
SYSTEMS GROUP
ONE SPACE PARK • REDONDO BEACH • CALIFORNIA

UNCLASSIFIED

Security Classification

DOCUMENT CONTROL DATA - R & D

(Security classification of title, body of abstract and indexing annotation must be entered when the overall report is classified)

1. ORIGINATING ACTIVITY (Corporate author)	2a. REPORT SECURITY CLASSIFICATION
TRW, INC ONE SPACE PARK REDONDO BEACH, CALIFORNIA 90278	UNCLASSIFIED
	2b. GROUP

3. REPORT TITLE

MAGNETIC FIELD ANNIHILATION OF IMPULSIVE CURRENT SHEETS

4. DESCRIPTIVE NOTES *(Type of report and inclusive dates)*

Scientific Interim

5. AUTHOR(S) *(First name, middle initial, last name)*

C L DAILEY

6. REPORT DATE	7a. TOTAL NO. OF PAGES	7b. NO. OF REFS
31 May 1972	33	3

8a. CONTRACT OR GRANT NO	F44620-71-C-0031	9a. ORIGINATOR'S REPORT NUMBER(S)	18706-6001-T0-00
b. PROJECT NO.	9752-02		
c.	61102F	9b. OTHER REPORT NO(S) *(Any other numbers that may be assigned this report)*	AFOSR-TR-72-1307
d.	681308		

10. DISTRIBUTION STATEMENT

Approved for public release; distribution unlimited.

11. SUPPLEMENTARY NOTES	12. SPONSORING MILITARY ACTIVITY
TECH, OTHER	AF Office of Scientific Research (NAE) 1400 Wilson Boulevard Arlington, Virginia 22209

13. ABSTRACT

This report presents the results achieved to date from an experimental study of impulsive plasma acceleration in an inductive device. The geometry of the magnetic fields produced in this machine is such that plasma acceleration by means of a hydromagnetic wave, that converts field energy to kinetic energy, is expected to occur. The purpose of the experiment is to study this mechanism of plasma acceleration by magnetic field annihilation. The experimental data consist of measurements of the radial and axial magnetic field components as a function of time and location within the accelerator. A computer analysis of these data has been made and the results are presented as magnetic flux contour maps and contour maps of plasma current density which are calculated by the computer from the magnetic field data. The maps are also drawn by the computer.

Details of illustrations in this document may be better studied on microfiche.

DD FORM 1 NOV 68 1473

34 I

UNCLASSIFIED

Security Classification

14 KEY WORDS	LINK A		LINK B		LINK C	
	ROLE	WT	ROLE	WT	ROLE	WT
MAGNETIC FIELD ANNIHILATION						
INDUCTIVE-IMPULSIVE PLASMA ACCELERATION						
PULSED PLASMA THRUSTER						
M H D PROPULSION						

MAGNETIC FIELD ANNIHILATION OF IMPULSIVE CURRENT SHEETS

Interim Scientific-Progress Report

May 31, 1972

Prepared for

Air Force Office of Scientific Research
1400 Wilson Boulevard
Arlington, Virginia 22209

Contract No. F44620-71-C-0031

Prepared by C. L. Dailey

TRW SYSTEMS GROUP

CONTENTS

1. INTRODUCTION AND SUMMARY

This report presents the results achieved to date from an experimental study of impulsive plasma acceleration in an inductive device. The geometry of the magnetic fields produced in this machine is such that plasma acceleration by means of a hydromagnetic wave, that converts field energy to kinetic energy, is expected to occur. The purpose of the experiment is to study this mechanism of plasma acceleration by magnetic field annihilation.

The experimental data consist of measurements of the radial and axial magnetic field components as a function of time and location within the accelerator. A computer analysis of these data has been made and the results are presented as magnetic flux contour maps and contour maps of plasma current density which are calculated by the computer from the magnetic field data. The maps are also drawn by the computer.

2. DESCRIPTION OF EXPERIMENT

The wave mechanism for conversion of magnetic field energy to plasma kinetic energy has been described theoretically by Petschek[1] and observed experimentally by Bratenahl[2]. This process has been suggested as a possible explanation of the fast magnetic field annihilation that is observed to accompany solar flares. It is of practical interest primarily for pulsed plasma thruster application and may also be useful for controlled thermonuclear fusion.

2.1 BACKGROUND

Petschek's model which neglects ohmic dissipation, thermal pressure and viscosity, predicts a flux contour geometry as illustrated in Figure 1

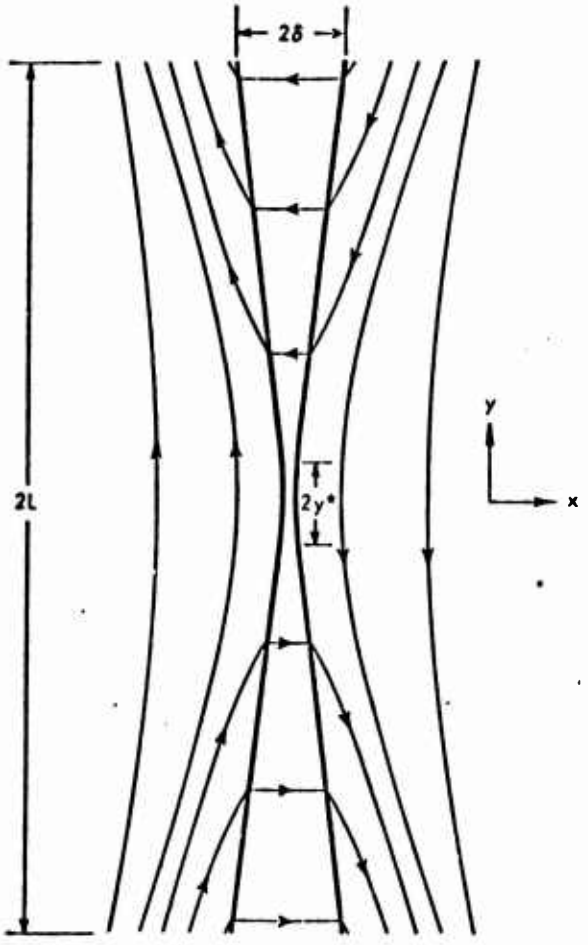

Figure 1. Petschek's Magneitic Field Annihilation Configuration

(this plot is reproduced from Reference 1). The plasma is assumed to approach the interaction layer with a velocity u_{xo} and a field strength B_{yo}. In the layer shown as 2δ this field has been reduced to zero and the plasma kinetic energy corresponding to a velocity v in the y direction

$$1/2\rho v^2 = \frac{(Byo)^2}{2\mu}$$

has appeared. Also in this region an x directed magnetic field Bx has appeared such that

$$1/2\ \rho u_{xo}^2 = \frac{Bx^2}{2\mu}$$

The linearly increasing width of the layer in the y direction accomodates the mass accumulation that also increases linearly with y.

In the length 2y* a finite conductivity σ is assumed so that B_x can change continuously through zero at the neutral point. In this region Petschek obtains the relation

$$B_x = -\,Byo\ 2y\mu\sigma V_A M_o^3$$

where

$$V_A = \frac{Byo}{\sqrt{\mu\rho}}$$

is the Alfvén speed

and

$$M_o = \frac{u_{xo}}{V_A}$$

is the Alfvén Mach number. He gives the scale of this zone as

$$y^* = \frac{1}{2\mu\sigma V_A M_o^2}$$

The above relations are expressed in MKS units.

In spite of the simplifying assumptions of the theory, the general feature of the magnetic field in Figure 1 showing the upward and downward pointing slingshot geometry characteristic of the Alfvén waves would be expected to appear in the accelerator. Accordingly the initial phase of the work reported here has been focused on obtaining a description of the magnetic fields during the first half-cycle of the discharge.

2.2 ACCELERATOR

The accelerator employs two 40 cm diameter flat spiral coils facing each other and spaced closely enough that each coil is inductively coupled to the plasma current at any location in the space between the coils. Each coil comprises 24, one-turn spirals of #14 copper wire extending from an O.D. of 40 cm to an I.D. of 10 cm. The wires are returned radially from the inner edge of the spiral to the outer edge where connections are made to 2 meter long RG8-U coaxial cables that separate the coils from the capacitor bank. The bank consists of 6, 4.5μf capacitors with a separate spark gap connected to each capacitor.

Figure 2 is a front view of one of the coils showing the spiral wires on the front surface and radial wires on the back side which are located two inches behind the spiral wires. The coil wires are covered with two 10 mil sheets of Mylar and a 1/16 inch thick annular glass disc with a 7.5 cm diameter hole at the center. The axial distance between the two glass covers is 3.62 cm., or about 9% of the coil diameter.

The coils are mounted in a small vacuum chamber. They are inserted through circular holes in square Lucite side plates as shown in Figure 2. These plates rest against an open steel framework with solid upper and lower steel plates and glass windows supported on O-ring seals on the sides. A side view of the assembly is shown in Figure 3. The glass covers are shown extending beyond the coil structure in this figure. They were later replaced by covers having the same O.D. as the coil.

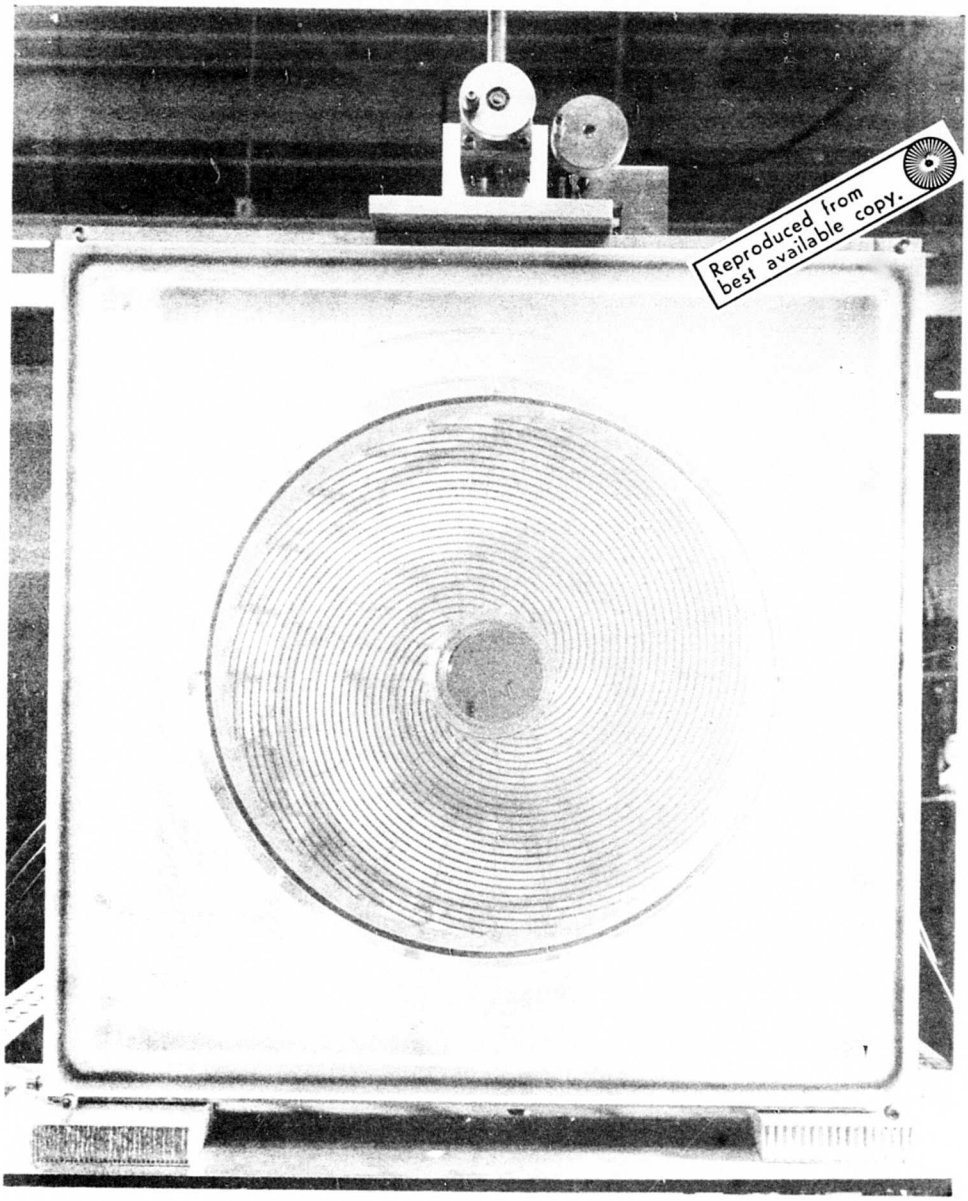

Figure 2. Front View of One of the Accelerator Coils

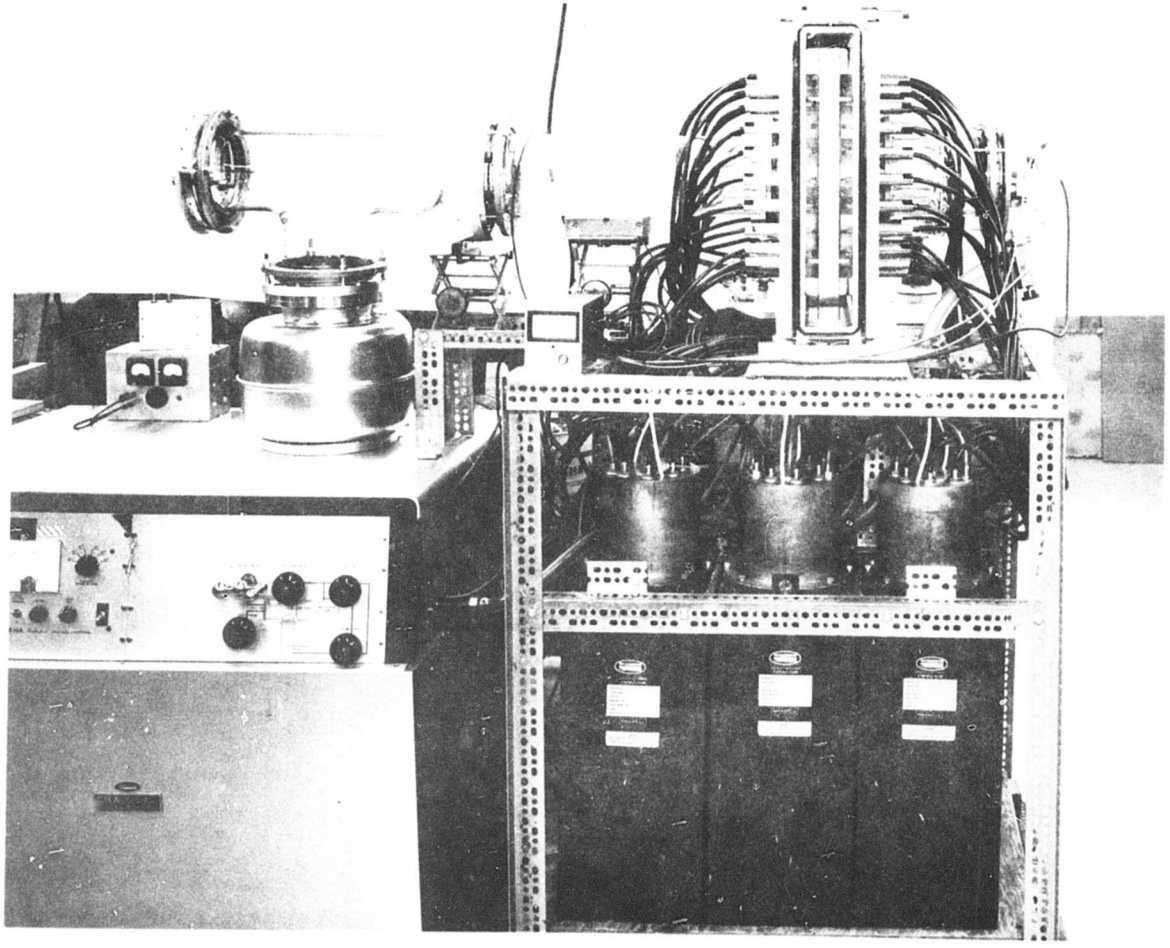

Figure 3. Side View of Coil Assembly Mounted Above Capacitor Bank

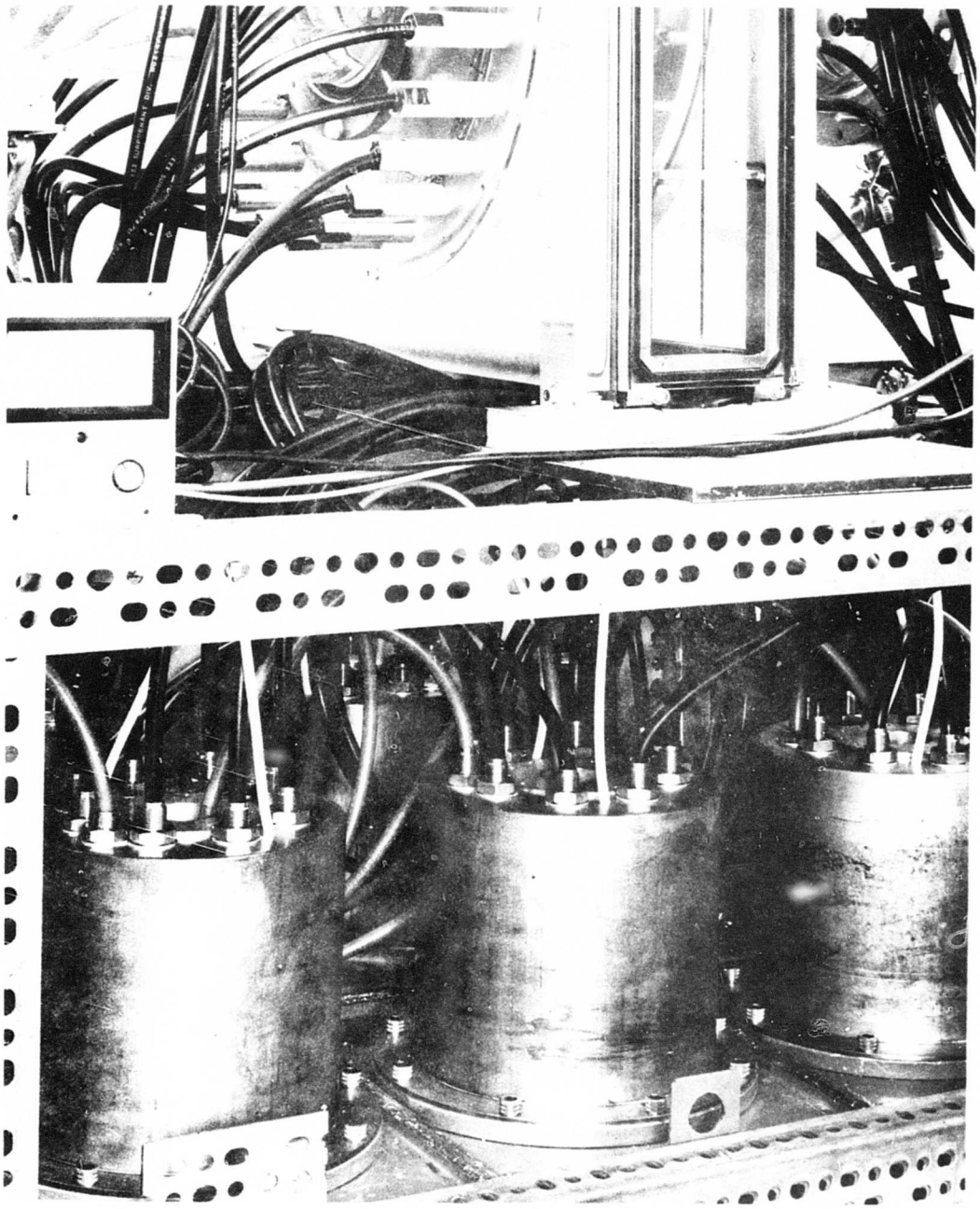

Figure 4. View Showing Cable Connections at Coil and Spark Gap Housings

As shown in Figure 3, the capacitors and spark gaps are located below the coils. A closer view in Figure 4 shows the cable connections. The white tubes shown in this figure circulate dry air through the gaps.

The accelerator is operated without preionization or crowbarring. For all of the work reported here, argon was used at 500 millitorr pressure. The bank voltage was 20 kv (5400 joules). At this voltage and pressure, a diamagnetic plasma current sheet formed with no observed delay as can be seen from the circuit current (lower trace) in Figure 5. The characteristic initially large rate of current rise followed by a reduced rate of fall at the end of the first half-cycle is evident. Another characteristic feature of the circuit current in pinch devices can also be seen in this figure. At about 2 μs after the current starts rising in each half-cycle there is a kink in the curve where dI/dt suddenly increases. At this time the individual planar plasma current sheets have collided at the mid-plane between the coils and the impedance due to the rate of inductance increase, which was positive, suddenly goes to zero. The associated voltage drop, I(dL/dt) must then be supplied by an increase in the other inductive voltage drop term, L(dI/dt). The upper trace in Figure 5 is Argon II light viewed along the axis of the accelerator (three shot overlay).

The region of maximum brightness appears to be a thin annular disc where the sheets of accelerated plasma collide at the mid-plane. This is illustrated in the time exposure photographs shown in Figures 6 and 7. This zone appears to be one to two mm thick and has a radial extent nearly the same as that covered by the coil wires.

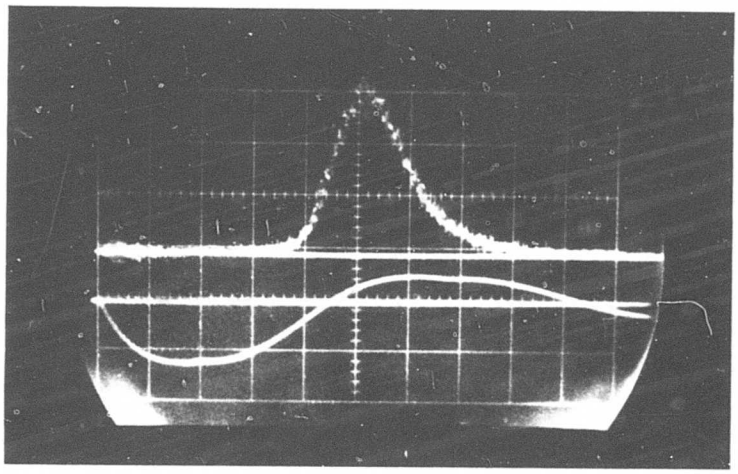

Figure 5. Oscillograph Traces Showing Circuit Current (Lower) and Argon II Light (Upper). Three traces overlay, 1 μs/cm sweep speed.

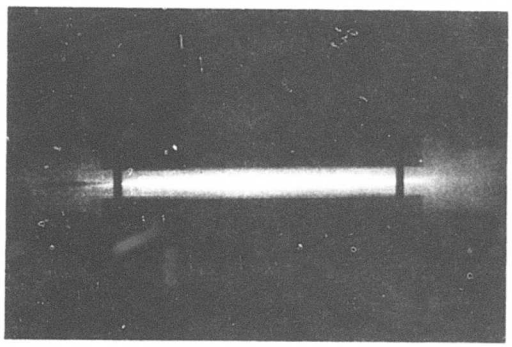

Figure 6. Time Exposure of Discharge—Side View

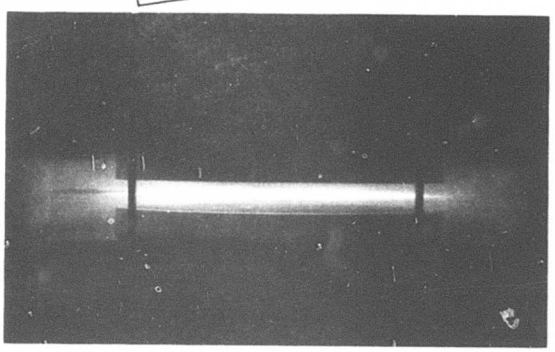

Figure 7. Time Exposure of Discharge—Inclined View Showing Dark Center Disc

3. RESULTS

The initial series of experiments has consisted of magnetic field measurement only. Some preliminary effort has gone into an attempt to measure charge separation electric field components in the axial and radial directions; but the results have been unsatisfactory because of noise and high frequency ringing that obscures the data for the first one to two μs. Because the magnetic field data are integrated, they are unaffected by oscillatory noise and a clean reliable mapping has been possible. Measurement of electric fields and other diagnostics will be carried out during the next year.

3.1 MAGNETIC FIELD MEASUREMENTS

The magnetic field measurements were made with a miniature probe located at the tip of a glass tube that was introduced into the plasma from the top of the chamber and extended parallel to the coil surfaces. The probe shaft therefore ran parallel to the plane of the plasma current sheet. The probe carriage, which permitted continuous positioning both axially and vertically (radial) can be seen at the top of the vacuum chamber in Figure 2. The probe itself is visible in Figures 6 and 7 where it is located at the mid-plane in the thin region of maximum brightness.

A check on possible interference from the probe shaft was made by two sets of data, one with a 6 mm diameter glass tube and the other with a 3 mm diameter glass tube. The probes were individually calibrated and the measurements were made two months apart. Spot checks of the results showed agreement to within ±5%. While this provides confidence in the repeatibility of the device and measurement technique it does not eliminate the possibility that the probe shaft might have interfered with the current sheet.

3.1.1 Magnetic Field Probes

The probes used in the 6 mm diameter glass tubing consisted of 20 turns with a 2 mm diameter window. The second pair of probe coils were about half this dimension in the axial and circumferential directions. In order to retain sensitivity they were extended about 8 mm in the radial direction. This was felt to be acceptable since radial variations in this

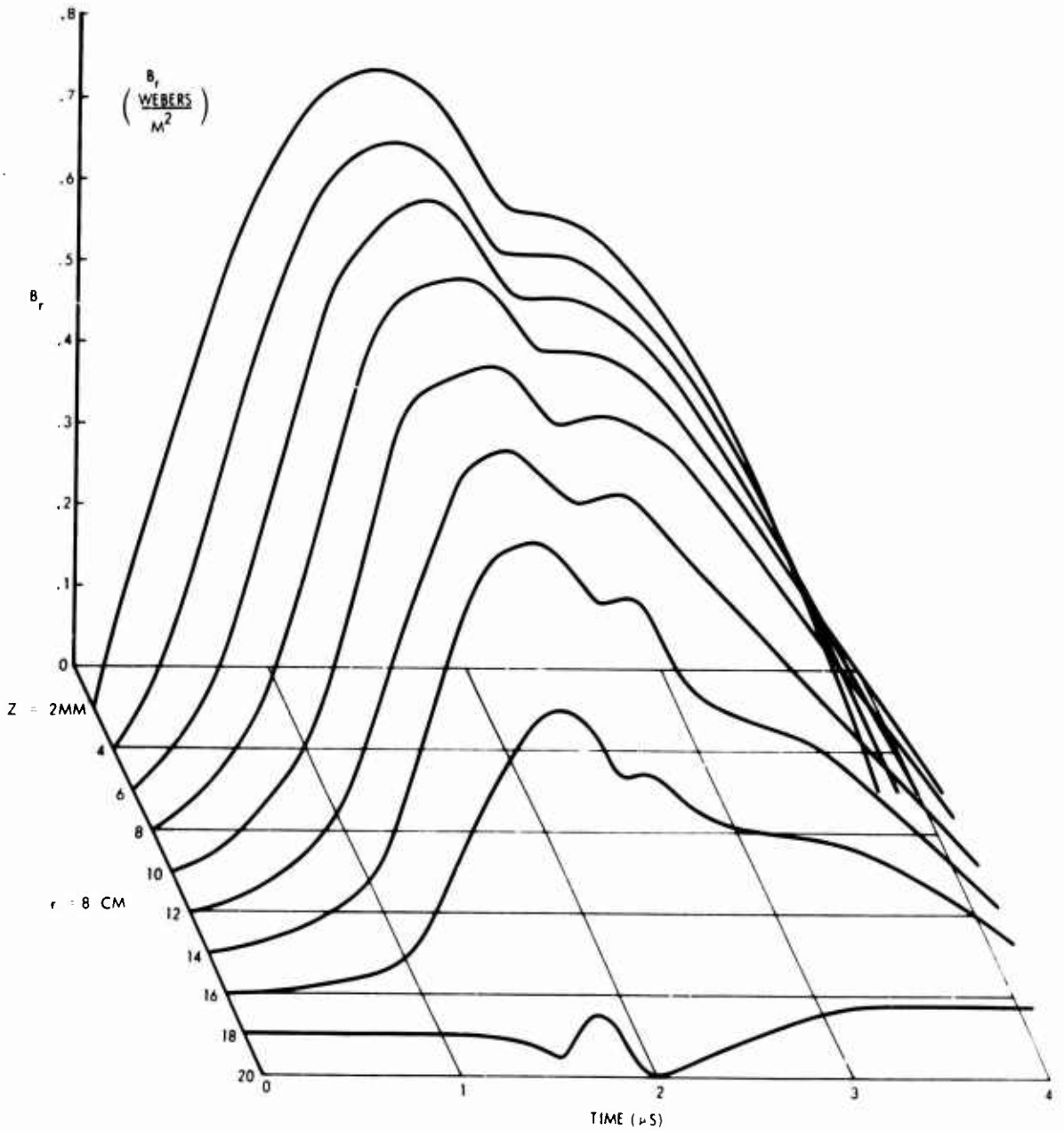

Figure 8. Radial Magnetic Field as a Function of Axial Position and Time for 8-cm Radius (R_{max} = 20 cm)

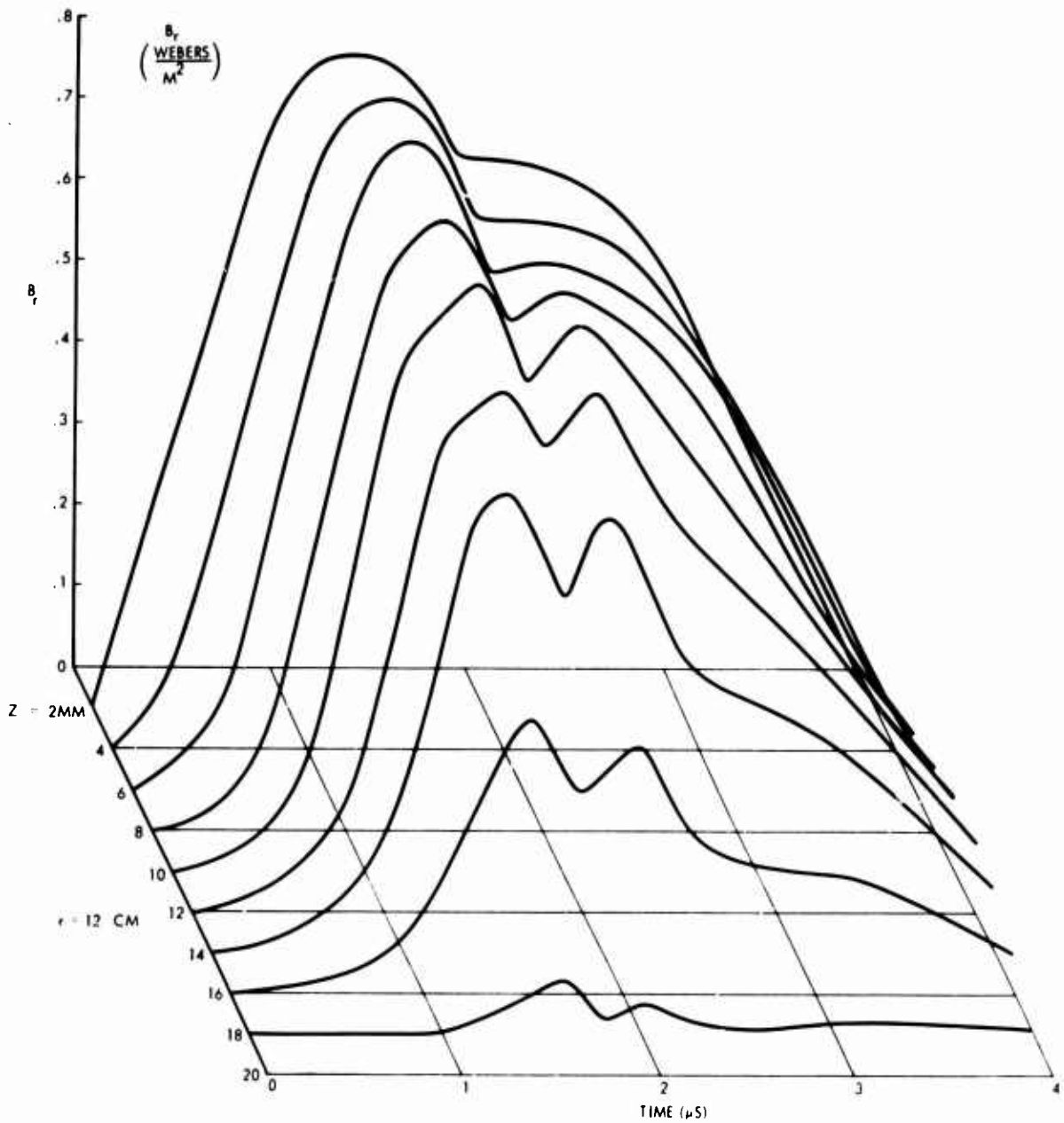

Figure 9. Radial Magnetic Field as a Function of Axial Position and Time for 12-cm Radius (R_{max} = 20 cm)

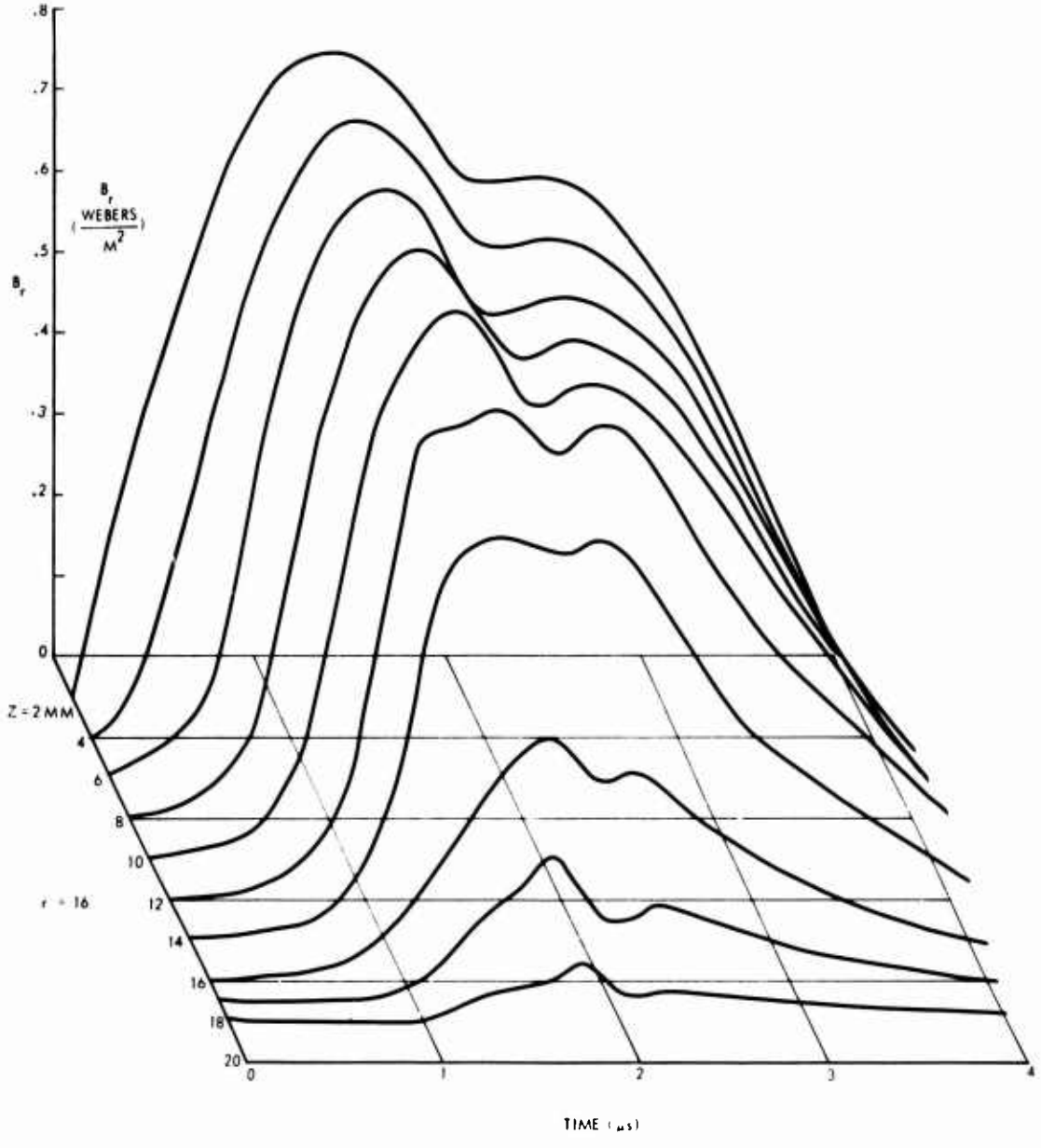

Figure 10. Radial Magnetic Field as a Function of Axial Position and Time for 16-cm Radius (R_{max} = 20 cm)

accelerator geometry are small compared to axial ones and there are no gradients in the circumferential direction.

The coil geometry of the axial magnetic field probe was a rectangle 1 mm wide in the circumferential direction and 9 mm long in the radial direction. The coil had 10 turns of #36 wire. The radial magnetic field probe was a one layer solenoid, 1 mm in diameter by 8 mm long in the radial direction, with 40 turns of #36 wire. The probes were calibrated with Helmholtz coils driven with a sinusoidal generator, the current being measured by a Hewlett-Packard Model 456 A current probe.

3.1.2 Magnetic Field Distribution

Magnetic probe data were recorded at a sweep speed of 0.5 μs/cm. The probes were terminated in 52 ohms at the oscilloscope and their signals integrated passively with a time constant of 100 μs. Data scans were made at 2 cm radial intervals and 2 mm axial intervals. The resulting oscilloscope traces were read and plotted directly as functions of time with axial position as parameter for each radial station. Radial Magnetic field plots are shown in Figures 8, 9, 10, and 11 for radial stations of 8, 12, 16 and 20 cm.

Axial distributions can be visualized in these figures as the intersection with the data plots of vertical planes passing through the constant time lines. For times up to about 1.5 μs, the propagating magnetic field typical of the single coil accelerator can be seen. About 1 μs is required for the toe of the field distribution to reach the midplane at 18.1 mm. At about 1.6 μs the field lines begin to drop and reach minimum at about 2 μs. This time corresponds to the sudden rise in dI/dt, shown as the kink in circuit current in Figure 6, that presumably occurs when plasma layers collide at the midplane. It is interesting that this event occurs at virtually the same instant over the entire axial length of the accelerator, i.e., no time is required for propagation.

Another interesting feature of the radial magnetic field plots is the linear decrease in B_r with z after the separate current sheets have coalesced into a single one. Petschek's illustration in Figure 1 shows a finite region at the mid-plane where $B_r = o$ and the field energy stored in B_r has already been converted to kinetic energy. The present data do not

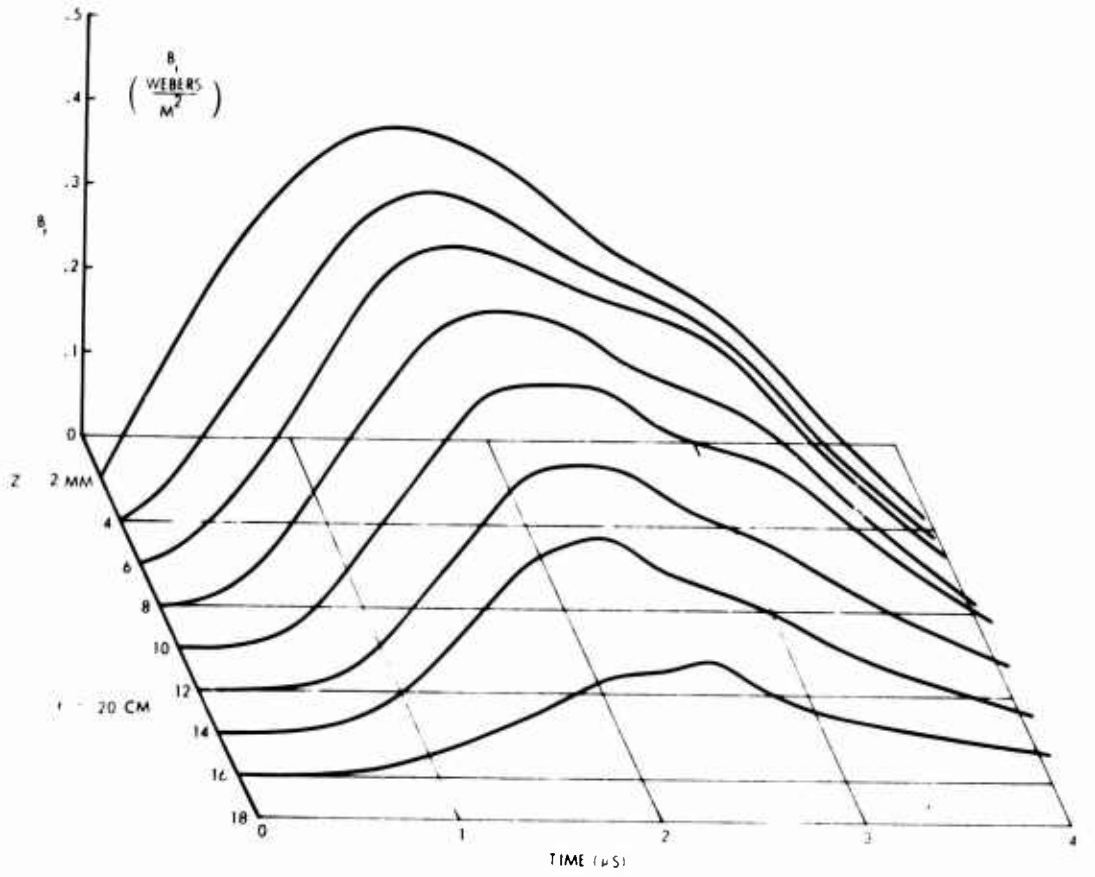

Figure 11. Radial Magnetic Field as a Function of Axial Position and Time for 20-cm Radius (R_{max} = 20 cm)

show such a region. B_r decreases linearly with z all the way to the mid-plane.

The general magnitude of the radial magnetic field is comparable for radial stations of 8, 12, and 16 cm, but has decreased noticeably at the 20 cm station. The 16 cm radial station is the neutral point (or circular ring) where Bz = o. It is not only the neutral point of the fully developed field configuration (usually a consequence of being the locus of initial collision of the two sheets) but is also the location of Bz = o for the separate axially accelerating current sheets as a consequence of the coil geometry which produces a maximum radial magnetic field at this radius.

3.2 CURRENT DENSITY MEASUREMENTS

In other investigations, current densities have been measured with Rogowsky probes and the results have seemed to agree with checks made

by calculating the current density from the curl of the magnetic field measurements.[3] The disadvantage of poor spatial resolution because of the large Rogowsky loop diameter is usually less serious than the time consuming operation of differentiating the magnetic probe data and the scatter that is intorduced by large changes in slope associated with small errors in field measurements. However, in this work, an attempt to improve resolution by using a very small Rogowsky probe seemed to give current readings that were lower than expected. Accordingly, current density data were obtained from the magnetic field data.

3.2.1 Current Density Distribution

A typical family of current density distributions is shown in Figure 12. This shows the current density as a function of axial station for different values of time at the 16 cm radius position. At 0.4 and 0.8 μs the distributions are typical of a single coil accelerator with a speed of about 1 cm per μs (10^4 m/s). At 1.2 μs the sheets have begun to merge at the mid-plane and at 2.0 μs the current density has risen to a maximum of 10,000 amps per cm^2, or about 50% more than the maximum of the individual current sheets. At this time the total current sheet thickness is a little more than one cm. The thickness increases slightly, but the current sheet remains concentrated near the mid-plane as it decays.

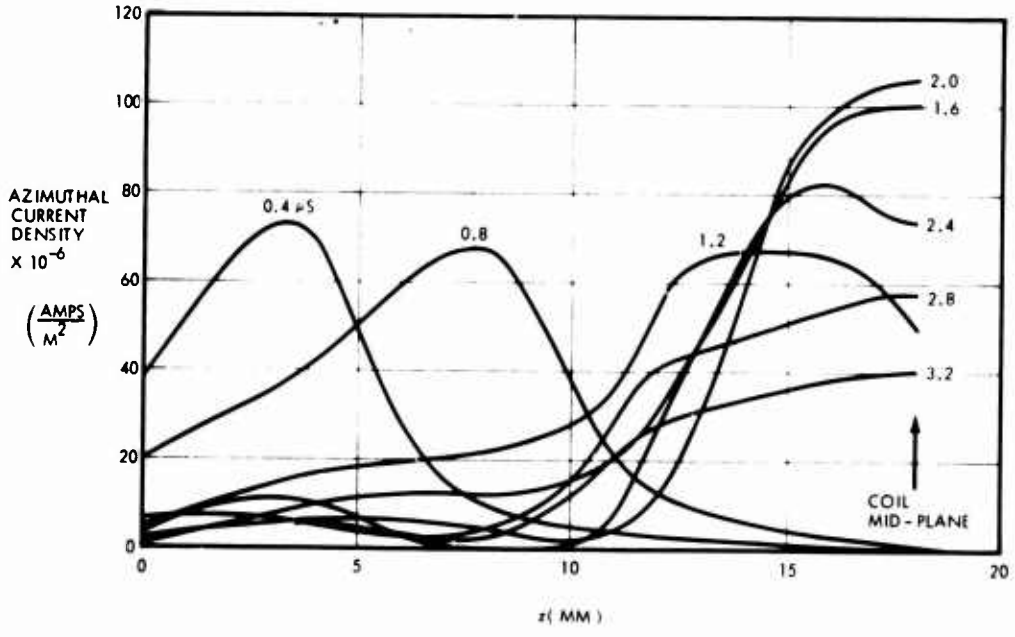

Figure 12. Plasma Current Density Distribution

3.3 COMPUTER DATA ANALYSIS

Flux plots, or maps of the magnetic field lines, are helpful in conveying an intuitive feeling of the accelerator operation. For example, the vacuum field in the space between the coils is essentially axial, so that deviations from an axial map of magnetic flux contour lines (i.e., lines of constant magnetic flux) are seen as the consequence of plasma currents. At early times, the plasma current sheets near the coil confine the magnetic field to the layer between each coil and its current sheet. Within this layer the resultant field is nearly radial and the thickness of the layer grows with time as the current sheet moves toward the mid-plane.

Another interesting feature is the x-type neutral point which must appear at a radius of 16 cm and must have the same general appearance as Figure 1. The development of this x-type field configuration as time progresses, as well as the progress of the initial current sheets across the accelerator and the diffusion of field lines ahead of the current sheet would be very interesting to observe.

Unfortunately field line plotting by hand is very time consuming as is the calculation of current density from the magnetic field data, and extensive analyses of this kind have not seemed feasible in the past. This subject, however, looks quite different when viewed as a computer problem.

TRW has available a CDC 6400-6500 time sharing computer system with CalComp plotting facilities. The latter includes a subroutine for generating contour lines that pass through calculated coordinate sets which define the lines. This subroutine accomplishes magnetic flux mapping from a set of coordinates calculated from a program that follows the field lines by integration along a line whose slope is the ratio of the magnetic field components. Another subroutine generates contour lines from input data consisting only of values of the dependent variable (i.e., when the contour coordinates are not specified). This subroutine is used for plotting constant current density contours from calculated values at the r, z coordinates for each value of time.

A TRW proprietary program is useful in calculating the magnetic field derivatives needed for computing the current density. This program accepts a matrix of data points, Br (r, z) for example, and simultaneously

fits curves Br (z) and Br (r) through these points that have continuous first and second derivatives.

The availability of this computer and software capability made it feasible to undertake the data analysis presented here. The work was carried out by Mr. R. F. Kemp in the Electric Propulsion Department at TRW.

Once the computer has been pressed into service, and the experimental data have been fed to it at sufficiently close space and time steps to obtain a useful result at any given instant in time, the next obvious step is to ask for output results at enough time values to make a motion picture. The output from the computer, for any time value, is then a tape containing instructions for either a Cal Comp plot on a sheet of paper or a plot made directly on a 35 mm film. There are two tapes for each time value, one for the magnetic flux plot and the other for the current density contours.

This has been done and a motion picture film has been prepared that shows the flux contours and current density contours on two separate plots that are displayed side by side. This result is thus similar to the familiar motion picture presentation of theoretical computer analyses and differs principally in that it uses experimental data as the input.

This difference is non-trivial and is especially difficult when the data values are used to define slopes as well as ordinates. The spatial intervals of the original probe measurements were 2 cm in the radial direction and 2 mm in the axial direction as already mentioned. This is a matrix of 110 test shots each for the radial and axial magnetic fields. These 220 oscilloscope traces are plotted and faired to make consistent families at each radial station like those shown in Figures 8 through 11. These data are then read at 0.1 μs intervals and input to the computer. This is a total of 40 time steps for 220 plots or 8800 input data values. The final key punched values are then printed out, examined for inconsistenties and edited. Several plots were made at selected times and examined for errors before the final output tapes were generated. An error in magnetic field at a single point has an ignorable effect on the flux contours but has an enormous effect on the current density plots because the computer puts a curve with continuous first and second derivatives through the bad point.

Consequently the current density is seriously in error and the final contour plots show meaningless mountains and valleys at the corresponding time frame. A few errors of this sort have escaped editing and appear on the film. In preparing the plots shown in Figure 12, some fairing to eliminate effects of this nature was done.

Further work could be done to improve the consistency of the data, for example by using computed values of the magnetic field divergence not only to indicate reading and key punching errors but as a guide in smoothing the data to obtain consistent slopes. However time did not permit further work in the present contract period.

3.3.1 Magnetic Flux and Current Density Contour Maps

Lines of constant magnetic flux and constant current density were plotted as parameters for the motion picture film. It is the motion of these lines through the accelerator that portrays the time history of current development and plasma motion.

At early times little magnetic flux has developed and consequently few contour lines are shown. A few additional plots have been made at selected times to convey a better feeling of the current sheet geometry. These are shown in Figure 13 for times of 0.2, 0.4, 0.8 and 2.0 μs. The first three time steps correspond to axial motion (see Figure 12) and the last is the time when the colliding sheets experience maximum current density, dI/dt of the circuit suddenly rises and the magnetic field plots (Figures 8 through 11) show a corresponding sudden rate of increase

The gradient of the magnetic flux (derivative normal to the contour lines) is proportional to the magnetic field strength. Thus the field strength is related to the closeness of lines and the field is strongest where the shades of grey due to convergence of the lines are darkest. The derivative of the gradient, or the rate of change of line spacing, is an indication of current density. The current density is large where shades of grey are changing rapidly and where the spacing between widely separated lines is decreasing.

In Figure 13 the contour lines are spaced at intervals of 0.0001, 0.0002, 0.00025 and 0.0003 Webers in the order of increasing time.

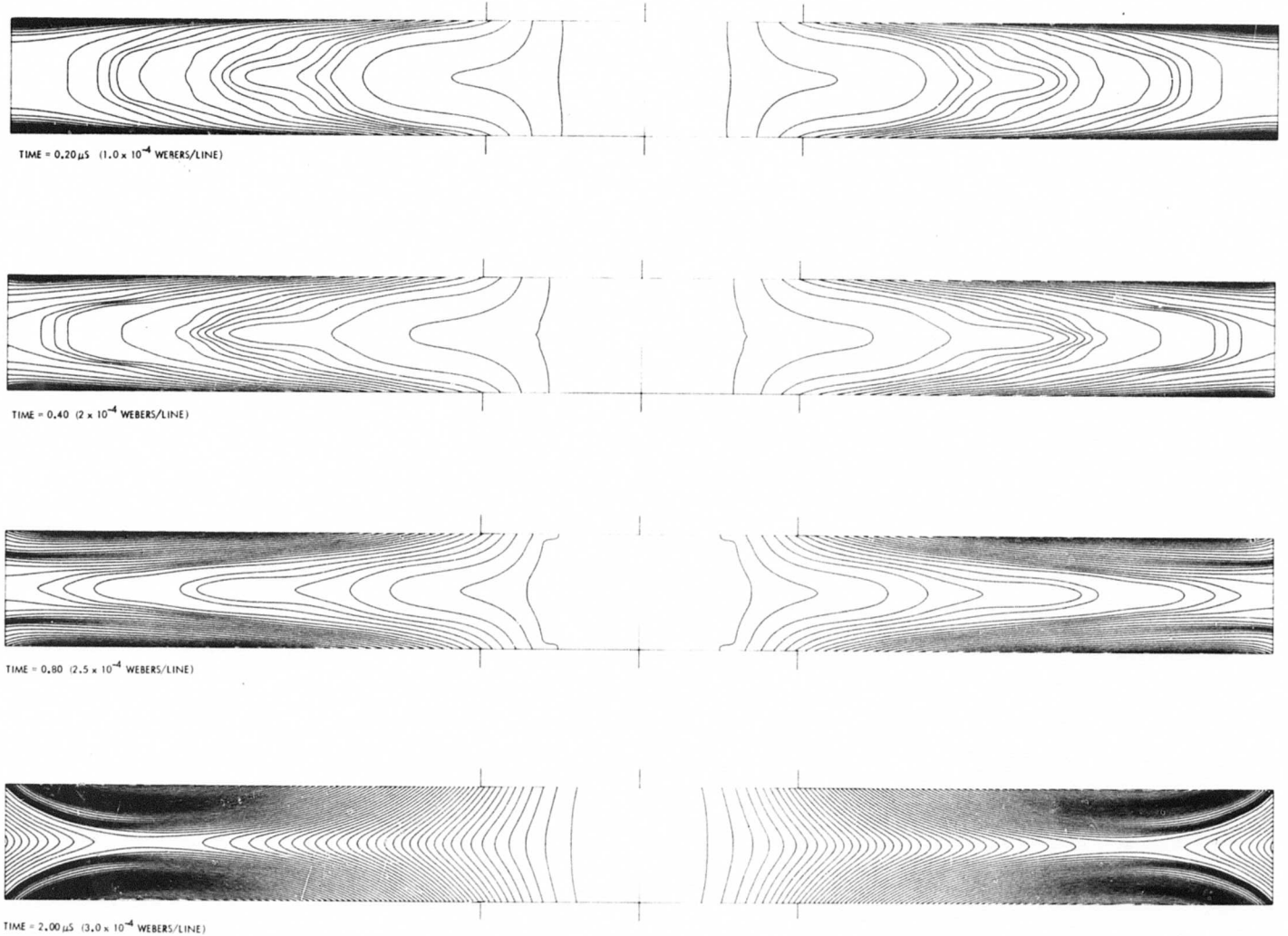

Figure 13. Magnetic Flux Contours for Different Times

The next 10 figures are frames from the motion picture. They cover a time span of 4.0 μs at 0.4 μs intervals (corresponding to the time intervals of Figure 12). The flux contours are 0.0005 Webers for all frames and the current density intervals are 5×10^6 amps/m^2 with zero corresponding to the heavy lines. The plot in each frame is current density and the lower one is magnetic flux.

4. CONCLUSIONS

Operation of the two-coil accelerator a 500 millitorr of argon and 5 kilojoules of stored energy has produced magnetic field configurations having the general features of the wave process of magnetic field annihilation described by Petschek. The X-type neutral point occurs at 80% of the radius.

Current densities calculated from the derivatives of the magnetic field data show axially propagating current sheets that collide at the midplane between the coils at a time of 2.0 μs. The peak current density after collision is 1.5 times the maximum in the sheets before collision.

Further diagnostic work is proceeding to obtain quantitative information about the acceleration mechanism. This includes measurement of axial and radial components of the charge separation electric field and spectroscopic measurements of line profiles to infur directed and thermal ion velocities as well as electron temperature measurements by means of line intensity ratios of AII lines.

5. REFERENCES

1. Petschek, H. E., "Magnetic Field Annihilation", Proceedings AAS-NASA Symposium on Physics of Solar Flares, NASA pp-50 (1965).

2. Bratenahl, A., and Yeates, C. M., "Experimental Study of Magnetic Flux Transfer at the Hyperbolic Neutral Point," Phys. Fluids, vol. 13, No. 11, pp 2696-2709 (1970).

3. Dailey, C. L., and Lovberg, R. H., "Current Sheet Structure in an Inductive - Impulsive Plasma Accelerator," AIAA Journal, Vol. 10, No. 2, pp 125-129 (1972).

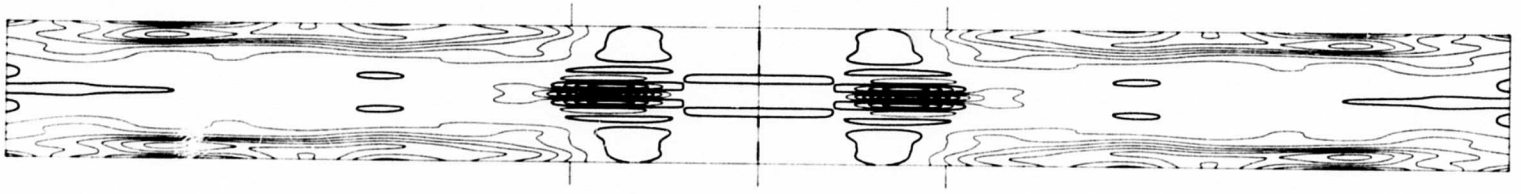

TIME = 0.40 μS

CURRENT DENSITY (5×10^6 AMPS/M^2 INTERVALS)

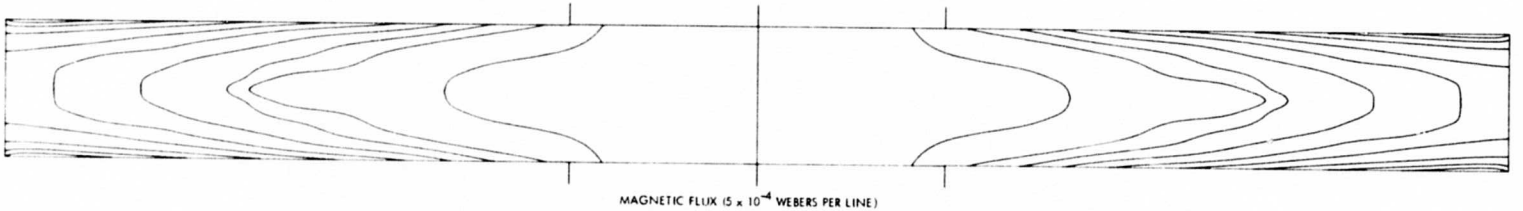

MAGNETIC FLUX (5×10^{-4} WEBERS PER LINE)

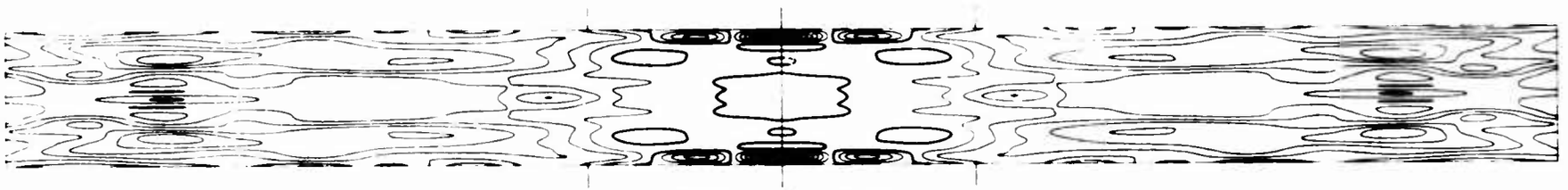

CURRENT DENSITY (5×10^6 AMPS/M^2 INTERVALS)

TIME = 0.80 μS

MAGNETIC FLUX (5×10^{-4} WEBERS PER LINE)

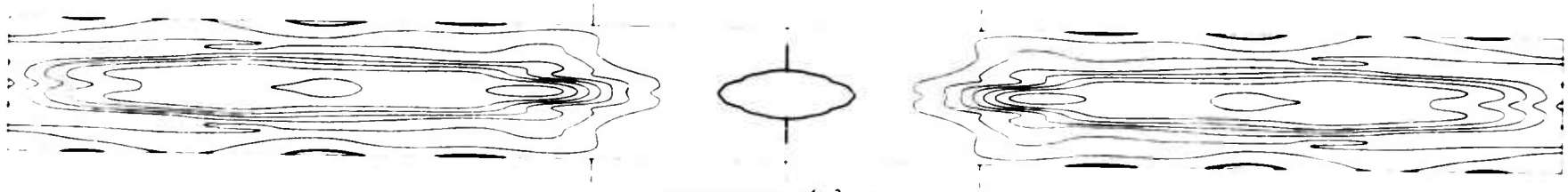

CURRENT DENSITY (5×10^6 M^2 INTERVALS)

TIME 1.20 μS

MAGNETIC FLUX 5×10^{-4} WEBERS PER LINE

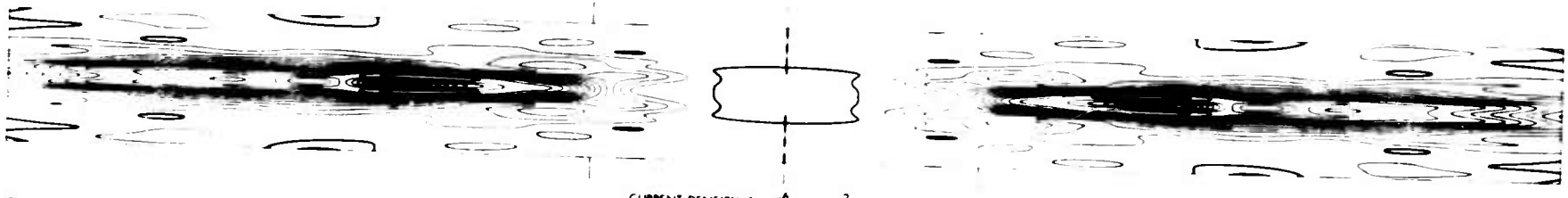

TIME 1.60 μS

CURRENT DENSITY (5×10^6 AMPS/M^2 INTERVALS)

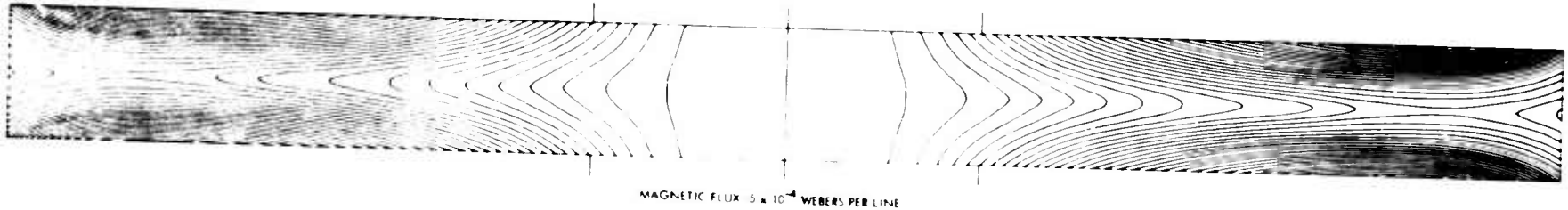

MAGNETIC FLUX 5×10^{-4} WEBERS PER LINE

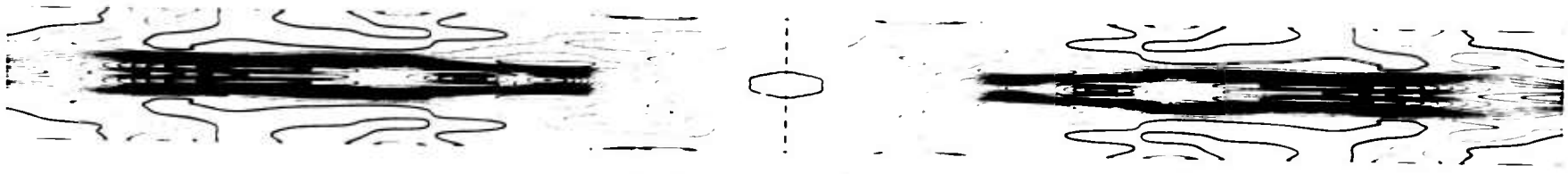

CURRENT DENSITY 5×10^6 AMPS/M^2 INTERVALS

TIME 2.00 μs

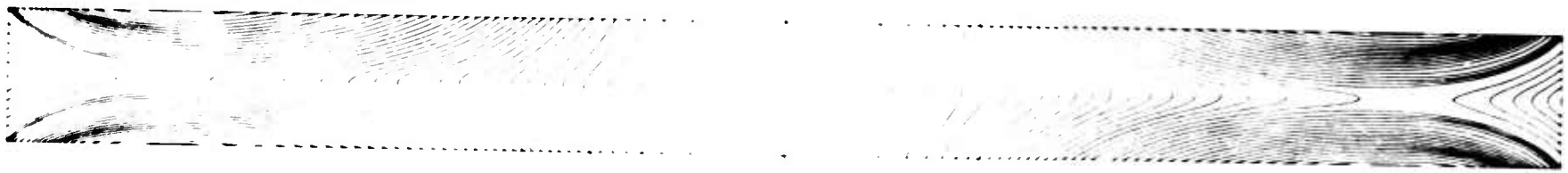

MAGNETIC FLUX 5×10^{-4} WEBER PER LINE

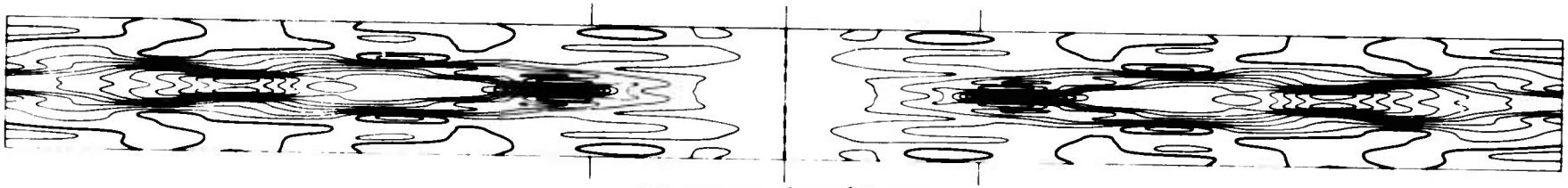

TIME = 2.40 μS

CURRENT DENSITY (5 × 10^6 AMPS/M^2 INTERVALS)

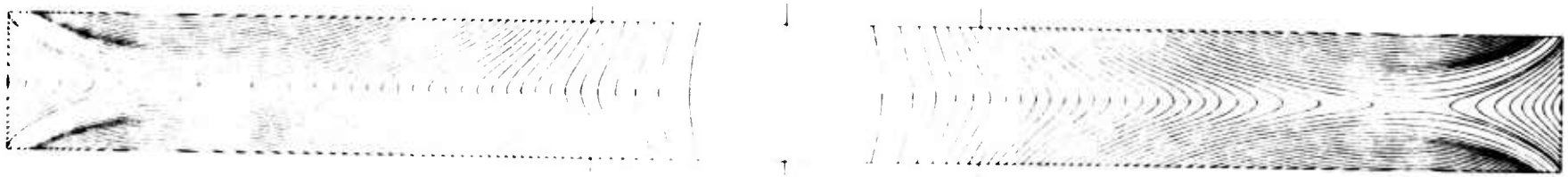

MAGNETIC FLUX (5 × 10^{-4} WEBERS PER LINE)

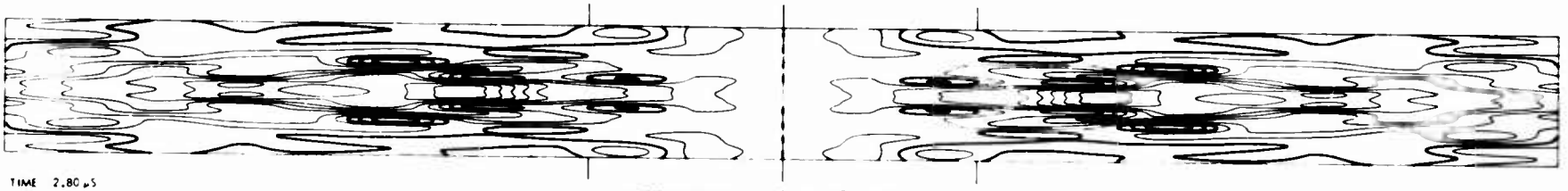

TIME 2.80 μS

CURRENT DENSITY (5 × 10^6 AMPS/M^2 INTERVALS)

MAGNETIC FLUX (5 × 10^{-4} WEBERS PER LINE

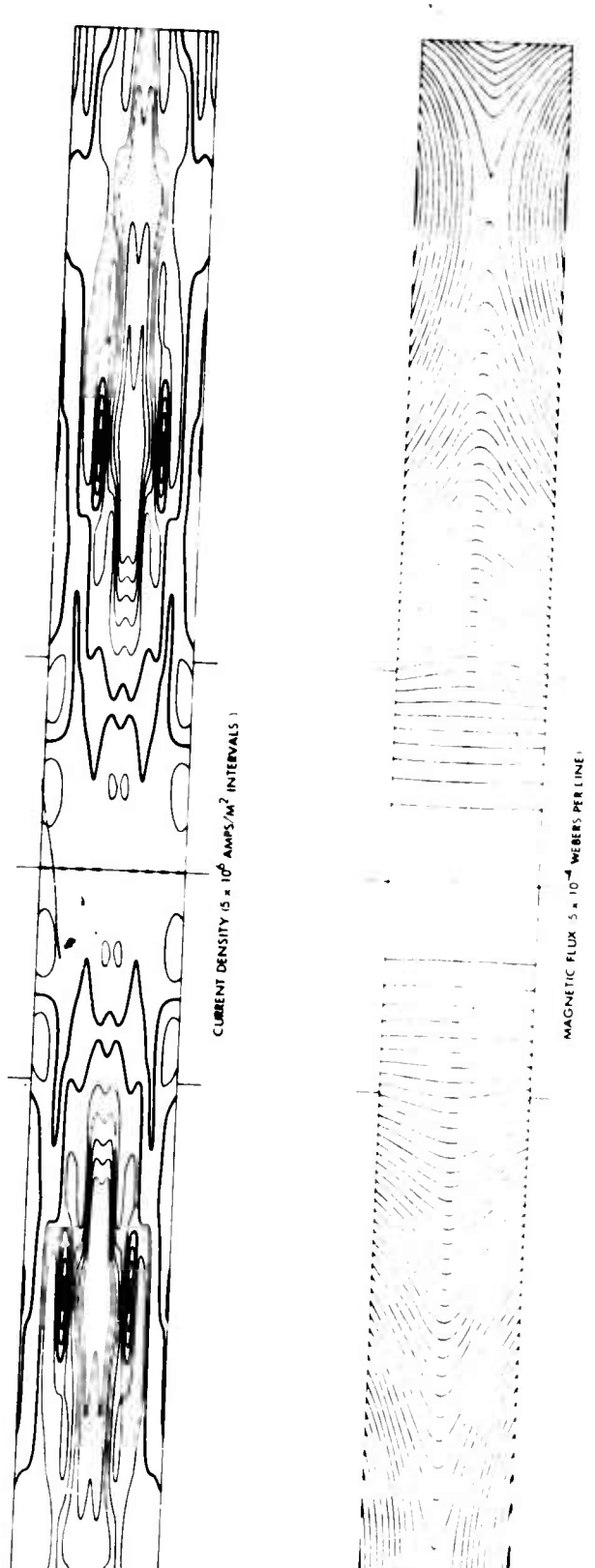
CURRENT DENSITY 15 x 10^6 AMPS/M^2 INTERVALS
MAGNETIC FLUX 5 x 10^-4 WEBERS PER LINE
TIME 3.20 μS

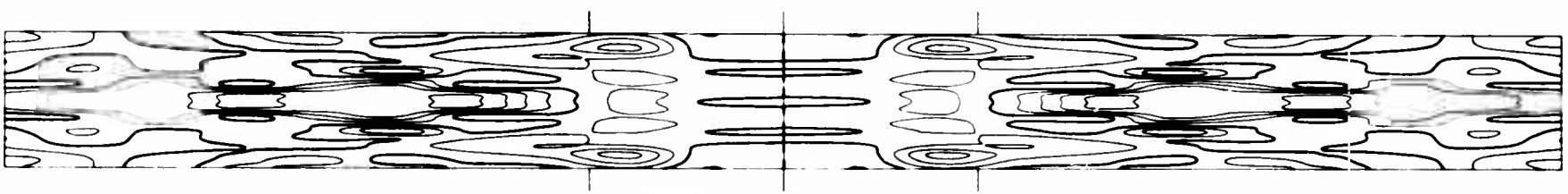

TIME 3.60 μS

CURRENT DENSITY (5 x 10^6 AMPS/M^2 INTERVALS)

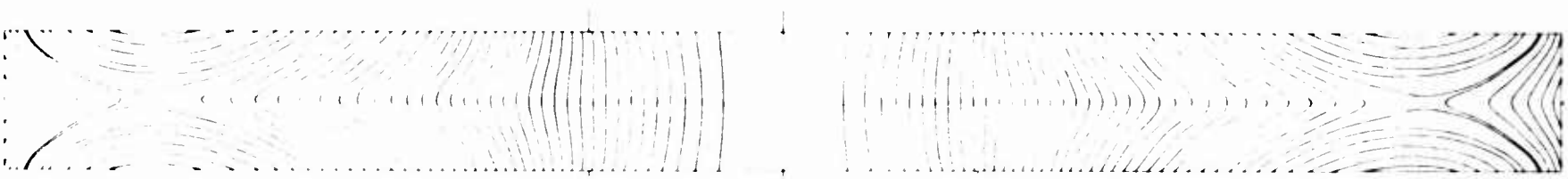

MAGNETIC FLUX (5 x 10^{-4} WEBERS PER LINE)

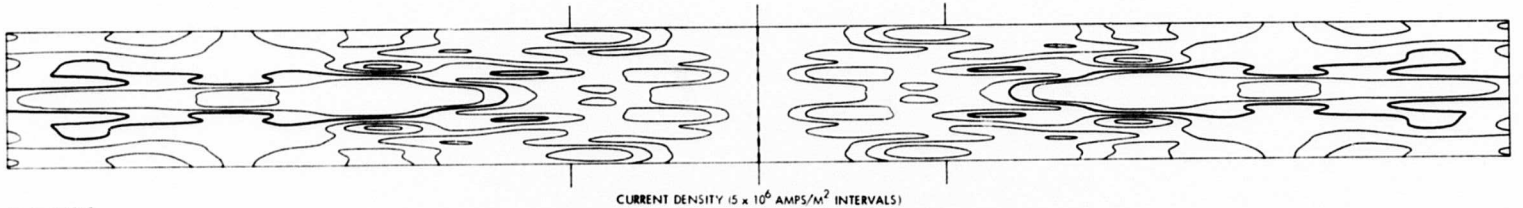

CURRENT DENSITY (5×10^6 AMPS/M^2 INTERVALS)

TIME = 4.00 μs

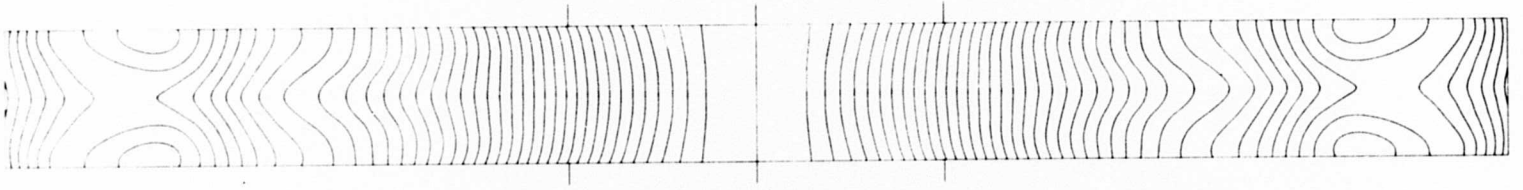

MAGNETIC FLUX (5×10^{-4} WEBERS PER LINE)